Mathematical Methods, Physical Methods and Simulation Science and Technology
Vol. 1 (2017)

Topological Horseshoe in a Simple 4D Hyperchaotic Oscillator

QINGDU LI

This paper studies hyperchaotic dynamics of a simple four dimensional circuit in terms of topological horseshoe. By means of interval analysis, two blocks are found in a carefully chosen 3D cross-section that can guarantee existence of a horseshoe for the corresponding second-return Poincare map on the both blocks expands in two directions. It justifiably indicates that there exists hyperchaos in the circuit.

1. INTRODUCTION

Hyperchaotic system is usually classified as chaotic system with more than one positive Lyapunov exponent, indicating that the chaotic dynamics of the system is expanding in more than one direction giving rise to a more complex attractor. So it is believed that hyperchaos can play a better role in most applied fields of chaos. In this way, hyperchaos has been studied with increasing interest in recent years, in the fields of nonlinear circuits [1, 2, 3, 4], secure communications [5], neural networks [6, 7], control [8] and synchronization [9, 10].

The existence of a horseshoe embedded in a dynamical system should be the most compelling signature of chaos, both in dissipative and conservative systems. Now it is recognized that horseshoe theory (Sample horseshoe or current topological horseshoe theory) with symbolic dynamics provides a powerful tool in rigorous studies of complicated dynamics such chaos in dynamical systems [11, 12, 13, 14, 15, 16]. This tool has been widely applied in the studies of the common chaos with one positive Lyapunov exponent [13, 17, 18]. However, due to the high complexity and high dimension of hyperchaos, to reveal the inside dynamics of hyperchaos with topological horseshoe theory is still a challenge.

Since Rössler introduced the first hyperchaotic system in [19], many systems have been proposed to exhibit hyperchaos [1, 2, 3, 4, 6, 7]. The simplest one among them should be the 4D hyperchaotic electronic circuit propossed in [3].

This system is not only simple in the circuit structure, but also simple in its dimensionless state equations which can be regard as switch system consisted of two simple linear systems.

In this paper, we revisit the electronic circuit, and present a 3D horseshoe numerically found in a certain Poincaré map. From this, a computer-assisted verification of hyperchaos in the circuit; is derived by virtue of topological horseshoe theory.

This paper is organized as follows: Section 2 recalls a result of topological horseshoe theory; Section 3 revisits the circuit; Section 4 presents discussions about the existence of hyperchaos in the circuit in terms of horseshoe; Section 5 draws conclusions.

2. A RESULT OF TOPOLOGICAL HORSESHOE THEORY

Before studying the hyperchaotic dynamics in the following sections, let us first recall a result on horseshoes theory, which is essential for rigorous verification of chaoticity of a chaotic system in terms of horseshoes.

Let X b a metric space, Q is a compact subset of X, and $f: Q \to X$ is map satisfying the assumption that there exist m mutually disjoint compact subsets $Q_1, Q_2, \ldots, Q_m$ of Q, the restriction of f to each Q_i i.e. $f|Q_i$ is continuous.

Definition 1: *Let γ be a compact subset of Q, such that for each $1 \le i \le m$, $\gamma_i = \gamma \cap Q_i$ is non-empty and compact, then γ is called a connection with respect to $Q_1, Q_2, \ldots, Q_m$ satisfying property: $\gamma \in F \Rightarrow f(\gamma_i) \in F$. Then F is said to be an f-connected family with respect to $Q_1, Q_2, \ldots, Q_m$*

Theorem 1: *Suppose that there exists on f-connected family with respect to $Q_1, Q_2, \ldots, Q_m$. Then there exists a compact invariant set $K \subset Q$, such that f/k is semiconjugate to m-shift dynamics.*

For details about the proof of this theorem, see [15], and for details of symbolic dynamics and horseshoe theory, see [11].

3. THE SIMPLE HYPERCHAOTIC CIRCUIT

The simple hyperchaotic circuit is shown in Fig. 1, which includes a combined parallel-series LC circuit, $L_1C_l - L_2C_2$. The opamp OA and the resistors R_1, R_3 and R_4 play the role of a negative impedance converter (NIC). For $R_3 = R_4$ the input impedance of the NIC is simply $-R_1$. The only nonlinearity is involved by the diode. The oscillator in Fig. 1 is described by the set of equations:

$$C_1 dv_1 / dt = \frac{v_1}{R_1} - i_1 - i_2$$

$$L_1 di_1 / dt = v_1 \tag{1}$$

$$L_2 di_2 / dt = v_1 - v_2$$

$$C_1 dv_2 / dt = i_2 - \tfrac{v_2 - v_0}{R_2} H(v_2 - v_0)$$

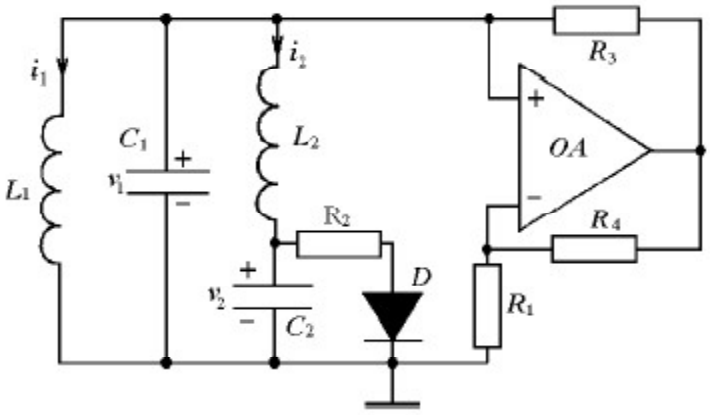

Figure 1: The fourth- order hyperchaotic

where v_1 and v_2 are the voltages acroos C1 and C_2, i_1 and i_2 denote the currents through L_1 and L_2, v_0 is the forward voltage drop of the diode, and $H(u)$ is the Heaviside function, i.e. $H(u < 0) = 0$ and $H(u \geq 0) = 1$.

By introducing the following notations:

$$x_1 = v_1 / v_0, x_2 = \rho i_1 / v_0, x_3 = \rho i_2 / v_0, x_4 = v_2 / v_0, t = t / \sqrt{L_1 C_1},$$

$$\rho = \sqrt{L_1 / C_1}, a = \rho / R_1, b = \rho / R_2, c = L_1 / L_2, e = C_1 / C_2,$$

we have the following dimensionless state eqautions of (1)

$$\begin{bmatrix} \dot{x}_1 \\ \dot{x}_2 \\ \dot{x}_3 \\ \dot{x}_4 \end{bmatrix} = \begin{bmatrix} a & -1 & -1 & 0 \\ 1 & 0 & 0 & 0 \\ c & 0 & 0 & -c \\ 0 & 0 & e & -h \end{bmatrix} \begin{bmatrix} x_1 \\ x_2 \\ x_3 \\ x_4 \end{bmatrix} + \begin{bmatrix} 0 \\ 0 \\ 0 \\ h \end{bmatrix}. \tag{2}$$

where $h = eb$ for $x_4 \geq 1$ and $h = 0$ for $x_4 \geq 1$.

A typical trajectory of the system is shown in Fig. 2 with the "classical" parameter values: $a = 0.7$, $b = 10$, $c = e = 3$ [3, 9 10]. The Lyapunove exponents comupted by the method proposed in [20] are approximately [0.119, 0.060, 0.000, –9.833]. Since the first two of them are positive and the sum of them is negative, there should exist a hyperchaotic attractor in the state space of the circuit. In order to verify the existence of hyperchaos, we will give detailed discussions about horseshoes imbedded in this attractor in the next section.

4. CROSS-SECTION AND POINCARJ MAP

Since (2) can be regarded as switching system consisted of two very simple linear subsystems, the Poincaré section plane just takes the switching hyperplane $P : x_4 = 1$ for the convenience of numerical computing by means of interval analysis, as shown in Fig. 2. The Poincaré map $\pi : P \rightarrow P$ is chosen as follows:

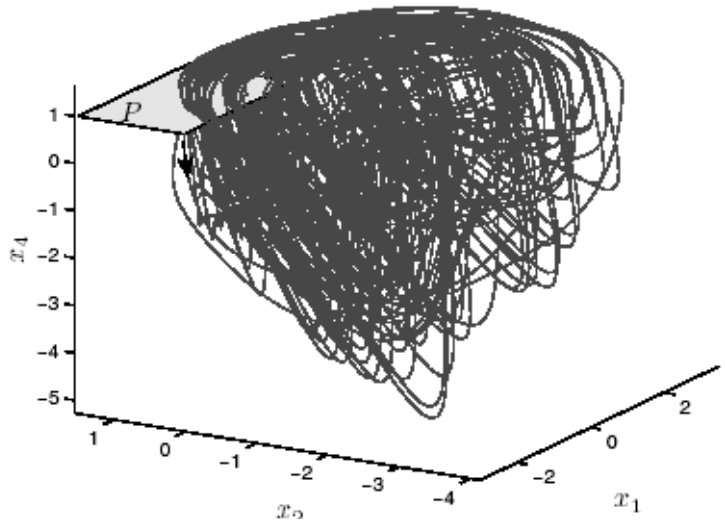

Figure 2: The phase plot of (2)

For each $X \in P$, $\pi(X)$ is taken to be the second return point in P under the flow with the initial condition X.

In order to seek a horseshoe, thousands of return points are calculated by interating with $X^{n+1} = \pi(X^n)$ from a random point in P, as illustrated in Fig. 3. It is easy to see from this figure that most of the return points are very close to a 2D plane, which means that the

expanding directions of the following Poincaré map almost parallel this plane. For clarity, we introduce the following coordinate transformation:

$$Y = HX, \text{ i.e. } [y_1,y_2,y_3,y_4]^T = H\,[x_1,x_2,x_3,x_4]^T \tag{3}$$

where H is a Householder matrix and

$$H = \begin{bmatrix} 0.99517608095718 & -0.00016242079179 & 0.09810474764354 & 0 \\ -0.00016242079179 & 0.99999453131088 & 0.00330317541594 & 0 \\ 0.09810474764354 & 0.00330317541594 & -0.99517061226805 & 0 \\ 0 & 0 & 0 & 1 \end{bmatrix} \tag{4}$$

so that the 2D plane parallels the plane *XOY*.

In the section hyperplane, we take two blocks (hexahedrons) by many attempts. The first one is a with its eight vertices in term of (y_1,y_2,y_3) to be

A_1 = (–0.767496277234, 0.675440856023, 0.110530023201),

A_2 = (–0.425820092816, 0.751530551862, 0.110530023201),

A_3 = (–0.422723329815, 0.538248828677, 0.110530023201),

A_4 = (–0.701431999884, 0.417197039842, 0.110530023201),

A_5 = (–0.767496277234, 0.675440856023, 0.090530023201),

A_6 = (–0.425820092816, 0.751530551862, 0.090530023201),

A_7 = (–0.422723329815, 0.538248828677, 0.090530023201),

A_8 = (–0.701431999884, 0.417197039842, 0.090530023201),

and the second one is *b* with its eight vertices in term of (y_1,y_2,y_3) to be

B_1 = (–1.119046544236, 0.723944393104, 0.110530023201),

B_2 = (–0.933088808164, 0.811254057430, 0.110530023201),

B_3 = (–0.894820978232, 0.742413745173, 0.110530023201),

B_4 = (–0.009026533183, 0.650066984829, 0.110530023201),

B_5 = (–1.119046544236, 0.723944393104, 0.090530023201),

B_6 = (–0.933088808164, 0.811254057430, 0.090530023201),

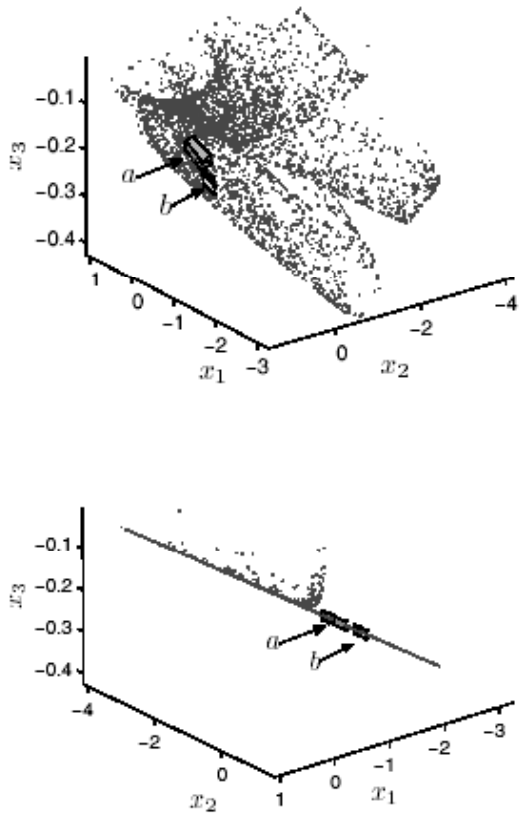

Figure 3: The return map of π from different view angles.

B_7 = (–0.894820978232, 0.742413745173, 0.090530023201),

B_8 = (–1.009026533183, 0.650066984829, 0.090530023201),

as shown in Fig. 3 and Fig. 4 For block a, it is easy to see that the top sursface $|A_1A_2A_3A_4|$ and the bottom surface $|A_5A_6A_7A_8|$ are parallel, and they are both quadrangular. The other four surface of *a* called the side of a in the following discussions (indicated with S_a) are all rectangular. For block *b*, it has the same situation with *a*, and the side of *b* is indicated with S_b.

Under the Poincaré map π, a is send to its image $a' = \pi(a)$ with

$$A_1' = \pi(A_1), A_2' = \pi(A_2), A_3' = \pi(A_3), A_4' = \pi(A_4),$$

$$A_5' = \pi(A_5), A_6' = \pi(A_6), A_7' = \pi(A_7), A_8' = \pi(A_8);$$

and b is send to its image $b' = \pi(b)$ with

$$B_1' = \pi(B_1), B_2' = \pi(B_2), B_3' = \pi(B_3), B_4' = \pi(B_4),$$

$$B_5' = \pi(B_5), B_6' = \pi(B_6), B_7' = \pi(B_7), B_8' = \pi(B_8).$$

Since each subsystem is linear, all solutions of the subsystems can be written in analytic formulas. Because the Poincaré map π can be regarded as a composition of four continuous sub-maps by the subsystems, it is easy to prove that for the block a or b all sub-maps are continuous, consequently, $\pi \mid Q$ is continuous.

By means of interval arithmetic [21, 22], each sub-map can be computed with estimating accuracy. Since a detailed interval analysis for the 3D Poincaré map will take incredible long time, we use a simplified method. Figure 5 and 8 are computed by sampling two millions of equally distributed points from the surface of a and b, that is, there is about one sample point for each 0.0003 × 0.0003 square. This takes a computer (Atholon XP 2.2 GHz) about 180 hours. The maximal global error is less than 3×10^{-40} for a, and 8×10^{-6} for b, which too small to be indicated in Fig. 5 and 8. From the two figures, we have the following statement.

Proposition 1 *For the Poincaré map p corresponding to the cross sections* $Q \stackrel{\Delta}{=} a \cup b$, there exists a closed invariant set $\Lambda \subset Q$ *for which* π / Λ *is semiconjugate to the 2-shift map.*

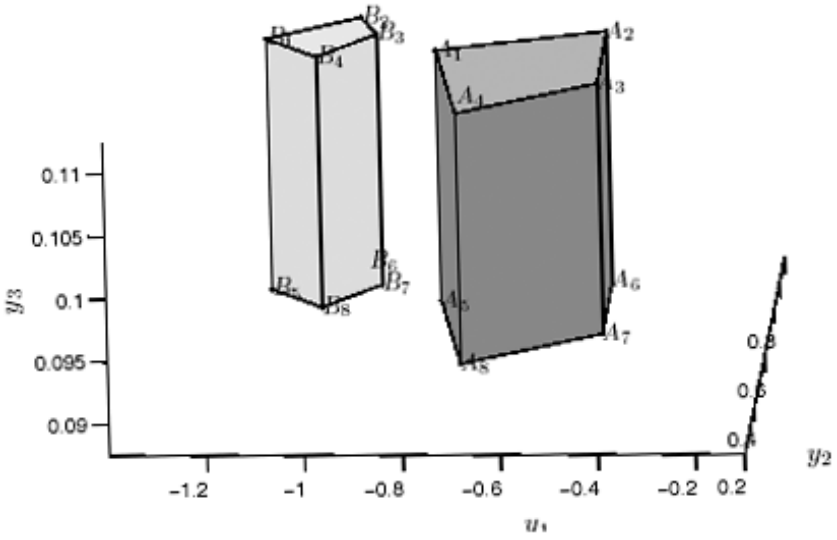

Figure 4: The position of block *a* and block *b*

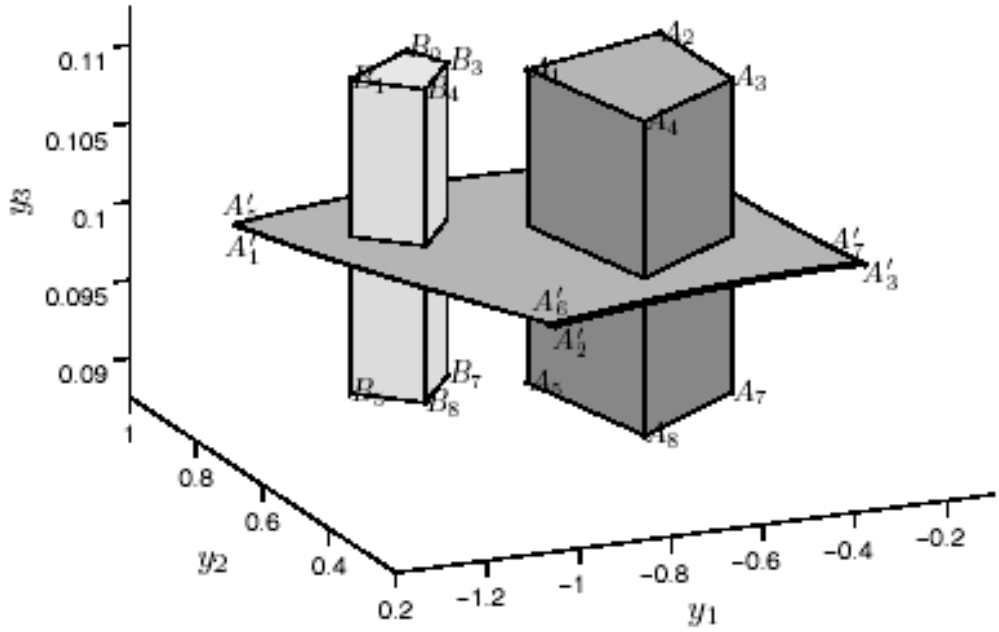

Figure 5: $a' = \pi(a)$ wholly across a and b

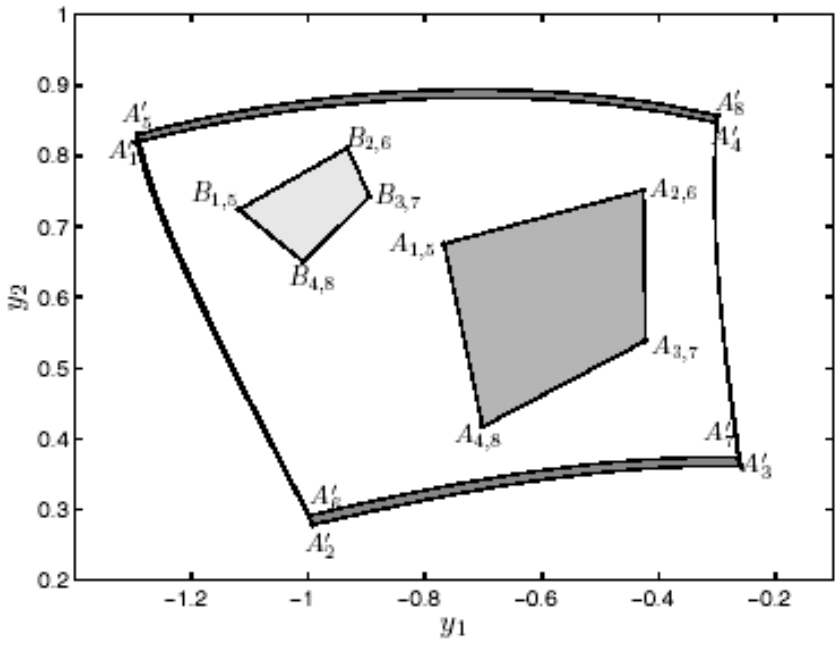

Figure 6: The top view of Fig. *5*.

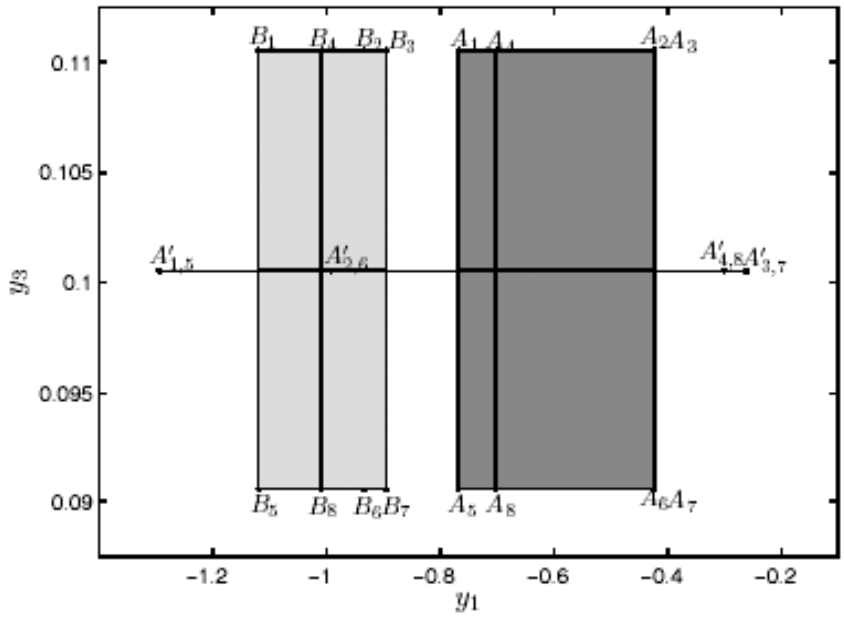

Figure 7: The side view of Fig. 5.

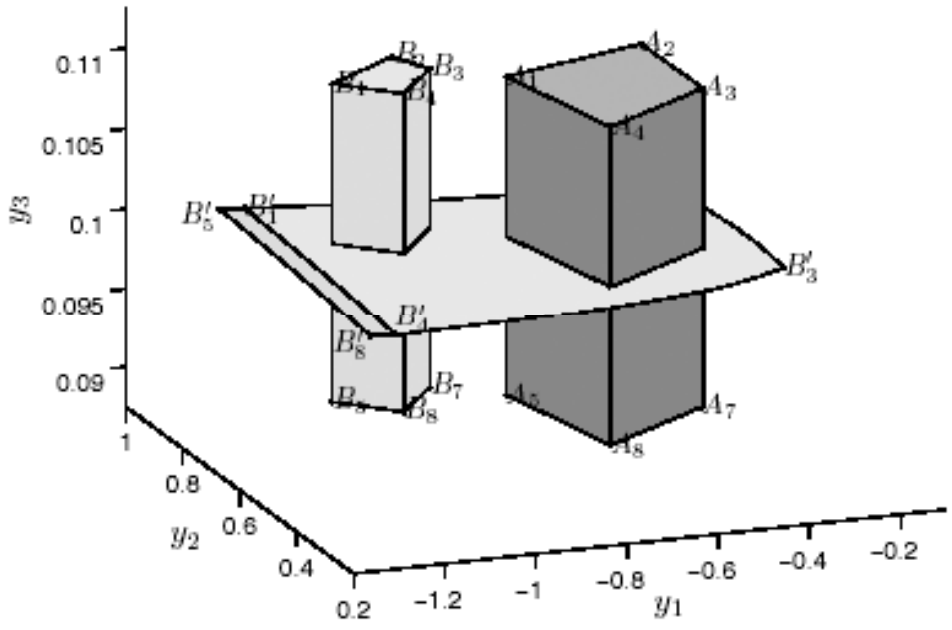

Figure 8: $b' = \pi(b)$ wholly across a and b

Proof: To prove this statement, we will find two disjoint compact subsets of Q, such that the existence of a π-connected family can be easily derived.

The first subset takes a as shown in Fig. 5, Fig. 6 and Fig. 7. From these figures, it is easy to see that the Poincaré map sends this subset to its image a' as follows:

- The top quadrangular $|A_1 A_2 A_3 A_4|$ and the bottom quadrangular $|A_5 A_6 A_7 A_8|$ are both expanded in two directions an wholly transversely intersect block a between $|A_1 A_2 A_3 A_4|$ and $|A_5 A_6 A_7 A_8|$ and block b between $|B_1 B_2 B_3 B_4|$ and $|B_5 B_6 B_7 B_8|$. The surface $|A_1' A_2' A_3' A_4'|$ is below the surface $|A_5' A_6' A_7' A_8'|$.
- The side of a, i.e. S_a, is mapped out side of S_a and S_b, as shown in Fig. 6.

In this case, we say that the image $a' = \pi(a)$ lies wholly across the blocks a and b with respect to the sides of a and b, i.e. S_a and S_b.

The second subset takes b as shown in Fig. 8, Fig. 9 and Fig. 10. The Poincaré map sends this subset to its image b' as follows:

- The top quadrangular $|B_1 B_2 B_3 B_4|$ and the bottom quadrangular $|B_5 B_6 B_7 B_8|$ are both expanded in two direction and wholly transversely intersect block a between $|A_1 A_2 A_3 A_4|$ and $|A_5 A_6 A_7 A_8|$ and block b between $|B_1 B_2 B_3 B_4|$ and $|B_5 B_6 B_7 B_8|$. The surface $|B_1' B_2' B_3' B_4'|$ is upon the surface $|B_5' B_6' B_7' B_8'|$.
- The side of b, i.e. S_b, is mapped out side of S_a and S_b, as shown in Fig. 9.

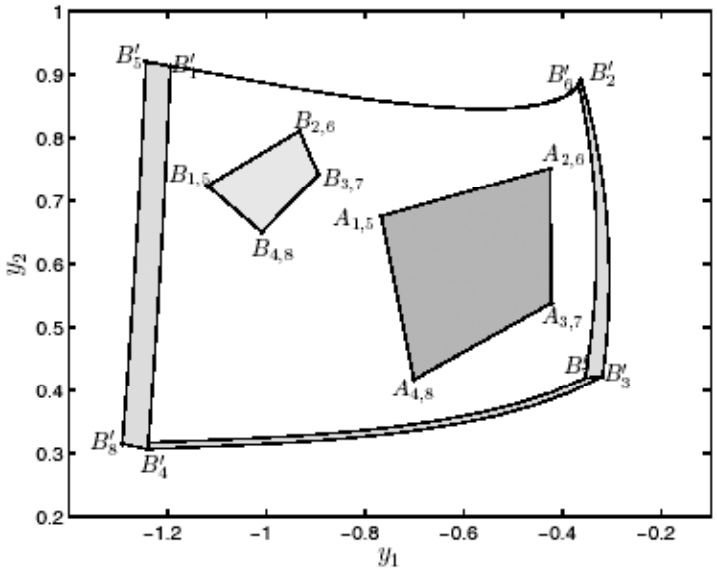

Figure 9: The top view of Fig. 8.

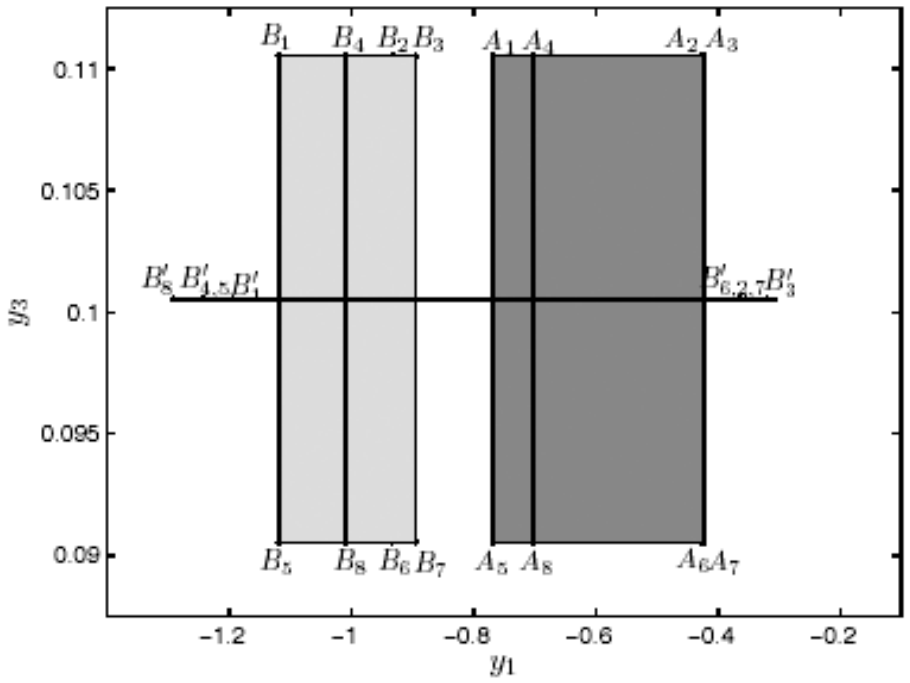

Figure 10: The side view of Fig. 8.

In this case, we say that the image $b' = \pi(b)$ lies wholly across the blocks a and b with respect to the sides of a and b, i.e. S_a and S_b.

Note that the subsets a and b are mutually disjointed. It is easy to see from the whole acrossness of $\pi(a)$ and $\pi(b)$ with respect to the both sides of a and b that there exists a π-connected family with respect to a and b. In view of Theorem 1, this means that the Poincaré map π is semiconjugate to 2-shift map.

The global picture of the images $\pi(a)$ and $\pi(b)$ suggests that $\pi \mid a$ and $\pi \mid b$ both expand in two directions. Thereby it justifiably indicates that the attractor illustrator in Fig. 2 is hyperchaotic.

5. CONCLUSIONS

This paper has presented a three dimensional horseshoe numerically found in a Poincaré map derived from the hyperchaotic circuit. By means of topological horseshoe theory, the hyperchaocity has been confirmed by computer assisted verification. This suggests an excellent methodology for study hyperchaos.

ACKNOWLEDGMENT

This work was partially supported by the Foundation for Young Teachers (A2005-15) and the Automation Project of Chongqing University of Posts and Telecommunications.

REFERENCES

[1] T. Matsumoto, L. O. Chua, K. Kobayashi, Hyperchaos: Laboratory experiment and numerical confirmation, IEEE Transactions on Circuits and Systems, **33** (11), 1143 - 1147, 1986.

[2] T. Saito, An approach toward higher dimensional hysteresis chaos generators, IEEE Transactions on Circuits and System I: Fundamental Theory and Applications, **37** (3), 399-409, 1990.

[3] A. Tamaševičius, A. Namajūnas, A. Cenys, Simple 4d chaotic oscillator, Electron Lett., **32** (11), 957-958, 1996.

[4] Y. Takahashi, H. Nakano, T. Saito, A simple hyperchaos generator based on impulsive switching, IEEE Trans. Circuit Syst. II, **51** (9), 468-472, 2004.

[5] V.S. Udaltsov, J.-P. Goedgbuer, L. Larger, W.T. Rhodes, Communicating with optical hyperchaos: information encryption and decryption in delayed nonlinear feedback systems, Physical Review Letters, **86** (9), 1892-1895, 2001.

[6] Q. Li, X.-S. Yang, Hyperchaos in hopfield-type neural networks, Neurocomputing, **67**, 275-280, 2005.

[7] Q. Li, X.-S. Yang, F. Yang, Hyperchaos in a simple CNN, International Jounal of Bifurcation and Chaos, in press.

[8] L. Yang, Z. Liu, J. min Mao, Controlling hyperchaos, phys. Rev. Lett., **84** (1-3), 67C70, 2000.

[9] G. Grassi, S. Mascolo, Synchronisation of hyperchaotic oscillators using a scalar signal, Electronics Letters, **34** (5), 424-425, 1998.

[10] D.A. Miller, G. Grassi, Experimental relization of observer-based hyperchaos synchronization, IEEE Transactions on Circuits And SystemsI: Fundamental Theory and Applications, 48 (3), 366-374, 2001.

[11] S. Wiggins, Introduction to Applied Nonlinear Dynamical Systems and Chaos, Springer-Verlar, New York, 1990.

[12] A. Szymczak, The conley index and symbolic dynamics, Topology, **35** (2), 287-299, 1996.

[13] J. Kennedy, J.A. Yorke, Topological horseshoes, Transactions of The American Mathematical Society, 353 (6), 2513-2530, 2001.

[14] P. Zgliczyński, M. Gidea, Covering relations for multidimensional dynamical systems, J. Diff. Equs, 202 (1), 33-58 2004.

[15] X-S. Yang, Tang, Horseshoes in piecewise continuous maps, Chaos, Soltions and Fractals , **19** (4), 841-845, 2004.

[16] X-S. Yang, Metric horseshoes, ChaoSolution & Fractlas, **20**, 1149-1156, 2004.

[17] P. Zgliczyński, Computer assisted proof of chaos in the rössler equations and in the hénon map, Nonlinearity, 10, 243-252, 1997.

[18] X.-S. Yang, H. Li, Y. Huang, A planar topological horseshoe theory with applications to computer verification of chaos, Journal of Physics A Mathematical and General, **38**, 4175-4185, 2005.

[19] O.E. Rössler, An equation for hyperchaos, Physics Letters A 71 (2-3), 155-157, 1979.

[20] J. P. Eckmann, D. Ruelle, Ergodic theory of chaos and strange attractors, Rev. Mod. Phys., 57, (3), 617-656, 1985.

[21] G. Alefeld, G. Mayer, Inetrval analysis: theory and applications, Journal of Computational and Applied Mathematics, **121** (1-2), 421-64, 2000.

[22] S.M. Rump, http://www.ti3.tu-harburg.de/rump/intalab/, 2005.

Qingdu Li
Institute for Nonlinear Systems
Chongqing University of Posts and Telecomm.
Chongquing 400065 China
Email: qingdu_li@163.com